JACS
JOURNAL OF THE AMERICAN CHEMICAL SOCIETY
pubs.acs.org/JACS
Article

Overestimated Halogen Atom Transfer Reactivity of α-Aminoalkyl Radicals

Weiqun Suo,[⊥] Jian-Qing Qi,[⊥] Jing Liu, Songtao Sun, Lei Jiao,* and Xingwei Guo*

Cite This: J. Am. Chem. Soc. 2024, 146, 25860−25869
Read Online
ACCESS | Metrics & More | Article Recommendations | Supporting Information

ABSTRACT: Halogen atom transfer (XAT) is a versatile method for generating carbon radicals. Recent interest has focused on α-aminoalkyl radicals as potential XAT reagents, previously reported to exhibit reactivity comparable to tin radicals. Utilizing an advanced time-resolved EPR technique, the XAT reactions between α-aminoalkyl radicals and organic halides were examined, allowing direct observation of the process through EPR spectroscopy and analysis of radical kinetics. Second-order rate constants for these reactions were determined, with some validated using transient absorption spectroscopy. The key finding is that the reactivity of α-aminoalkyl radicals in XAT reactions is 10^3 to 10^5 times lower than that of tin and silicon radicals and only slightly higher than alkyl radicals. This challenges the belief that α-aminoalkyl radicals are as reactive as tin radicals. The study on the solvent effect indicates that the XAT reaction of α-aminoalkyl radicals does not involve a highly polarized transition state, suggesting that the kinetic polar effect in this XAT process is not as significant as previously believed. The present study provides a reliable XAT reactivity scale for α-aminoalkyl radicals, which is crucial for designing XAT reactions and understanding their mechanisms.

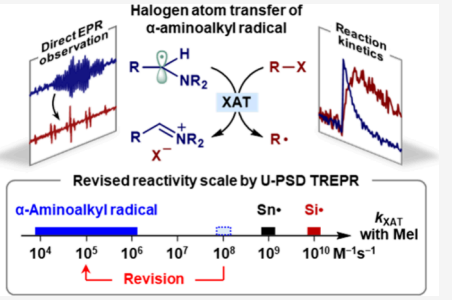

INTRODUCTION

Halogen atom transfer (XAT) reaction offers a reliable and versatile approach to carbon-centered radicals from easily accessible organic halides,[1,2] which has become a trusted tool for chemists.[3−5] Classical XAT reactions initiated by tin or silicon radicals exhibit great reactivity and excellent substrate compatibility. The introduction of visible-light photoredox catalysis[6−8] has greatly broadened the synthetic capabilities of chemists, allowing for the versatile generation of silicon radicals in XAT reactions.[9,10] Recently, there has been significant interest in exploring novel XAT reagents beyond traditional tin and silicon radicals, with one prominent example being the α-aminoalkyl radical (Figure 1A). Lalevée and co-workers first demonstrated that α-aminoalkyl radicals are able to undergo XAT with polyhalomethanes,[11−13] and the Doyle group utilized this chemistry to perform radical addition of halomethyl radicals to alkenes (Figure 1B).[14] More recently, the Leonori lab reported that α-aminoalkyl radicals could act as competent XAT reagents for the activation of normal alkyl and aryl halides (Figure 1C).[15] Since α-aminoalkyl radicals can be easily generated from abundant and inexpensive amines either via hydrogen-atom transfer (HAT) or by single electron oxidation/deprotonation, this approach allowed for XAT processes without using highly toxic and hazardous tin reagents, as well as accentuated the role of amines beyond mere electron donors in photoredox catalysis.

Remarkably, α-aminoalkyl radicals are believed to display a reactivity profile similar to that of classical tin radicals (Figure 1C). By using transient absorption (TA) spectroscopy/laser flash photolysis (LFP), Leonori and co-workers recently postulated that the XAT reaction (k_{XAT}) between the triethylamine-derived α-aminoalkyl radical and cyclohexyl iodide proceeds with a second order rate constant of 3.6×10^8 $M^{-1}s^{-1}$, similar to the XAT reactivity of the tributyltin radical (typical $k_{XAT} \sim 10^9$ $M^{-1}s^{-1}$).[15] This rate constant is significantly higher than that of ordinary carbon-centered radicals (e.g., k_{XAT} of the reaction between *n*-octyl radical and isopropyl iodide is 9.5×10^5 $M^{-1}s^{-1}$)[16] despite the greater radical stability of α-aminoalkyl radicals (e.g., the radical stabilization energy, RSE, of $Me_2NCH•Me$ is −54.6 kJ/mol).[17,18] The kinetic polar effect was postulated to play a vital role in enhancing the XAT reactivity of α-aminoalkyl radicals, which resembles the highly polarized XAT transition states involving silicon and tin radicals.[15] Thus, the α-aminoalkyl radical was postulated to be the very carbon-centered radical exhibiting XAT reactivity akin to traditional tin radicals.

In view of the great importance of α-aminoalkyl radicals, we performed a systematic investigation into their XAT reactivities by using our recently developed ultrawide single sideband phase-sensitive detection (U-PSD) time-resolved electron paramagnetic resonance (TREPR) technique,[19] which has been proven to be a powerful tool for investigating radical-

Received: July 18, 2024
Revised: August 27, 2024
Accepted: August 28, 2024
Published: September 5, 2024

https://doi.org/10.1021/jacs.4c09792
J. Am. Chem. Soc. 2024, 146, 25860−25869

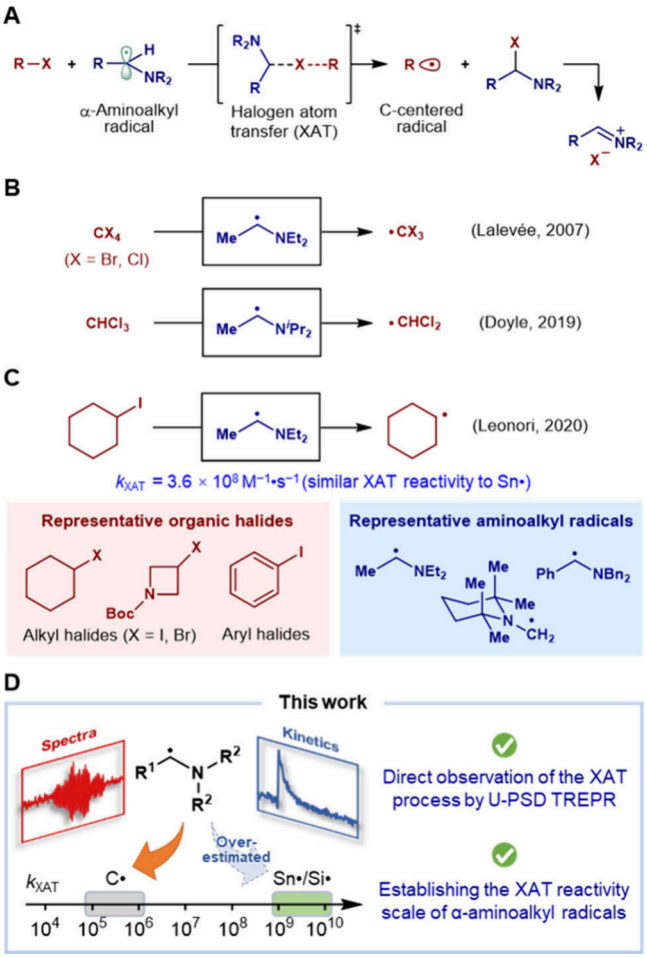

Figure 1. Halogen atom transfer (XAT) between α-aminoalkyl radicals and organic halides. (**A**) The model reaction. (**B**) The XAT reactions between polyhalomethanes and α-aminoalkyl radicals. (**C**) Recent discoveries on the XAT reactions of normal alkyl and aryl halides. (**D**) This work.

mediated mechanisms.[20] By directly observing the radical intermediates in the XAT process of various α-aminoalkyl radicals, we found that, in contrast to the previous report,[15] the α-aminoalkyl radicals are 10^3 to 10^5 times less reactive than the tributyltin radical, with the tribenzylamine-derived radical showing negligible reactivity. The experimental results in this study showed that the XAT reactivity of α-aminoalkyl radicals is largely overestimated, and the kinetic polar effect in this XAT process is not as significant as previously believed. As a consequence, the mechanistic interpretations based on the overestimated reactivity profile should be reconsidered (Figure 1D).

RESULTS AND DISCUSSION

1. Direct Observation of the XAT Process with U-PSD TREPR. The α-aminoalkyl radicals **R1**−**R5**, known for their good XAT reactivity according to the previous report, were selected as the focus of our investigation. Various organic halides **1**−**5**, including methyl, primary alkyl, secondary alkyl, tertiary alkyl, and phenyl halides, were chosen as the reaction partners. Additionally, *N*-Boc-3-haloazetidines **6** and **7**, which were most commonly used in the synthetic examples of previous XAT studies,[15,21−23] were also included. The α-aminoalkyl radical was generated through the photolysis of di-*tert*-butyl peroxide (DTBP) in the presence of the corresponding amine in an acetonitrile solution (Figure 2A).

TREPR Spectra. Using the U-PSD TREPR technique, we examined the interaction between **R1** and isoamyl iodide (**2**). Following the LFP at 355 nm, the transient EPR spectrum of **R1** was recorded within a delay of 0−5 μs (Figure 2B, blue spectrum). The spectral signature of **R1** reveals hyperfine splittings (HFSs) from both ^{14}N, α-C-H, and β-C-H (a_N = 0.53 mT, a_H = − 1.35 mT, $3a_H$ = 1.93 mT). These values are consistent with previously documented steady-state spectra of the α-aminoalkyl radical derived from triethylamine in an adamantane matrix.[24] The spectrum obtained in our solution phase studies shows a slight nuclear-dependent polarization, with enhanced absorption at high fields and reduced absorption at low fields. This observation aligns well with the free radical pair (F-pair) polarization mechanism, resulting from the superimposition of the emission/absorption (E/A) polarized spectrum and the Boltzmann-populated steady-state spectrum. The decay of **R1** and the emerging of a new radical species were evidenced by the evolving spectra ($2a_H$ = − 2.18 mT, $2a_H$ = 2.68 mT, a_H = 0.10 mT) at longer delays (Figure 2B, green and red spectra). This species was identified as the isoamyl radical based on its characteristic HFSs.

Reaction Kinetics. The time evolution of both radicals was monitored by observing the nonoverlapping peaks in their spectra (Figure 2C). These kinetic profiles, which show the simultaneous decay of **R1** and the generation of the isoamyl radical, further confirmed the presence of the elementary XAT process (see expanded subfigure in Figure 2C). Due to the inevitable self-termination of radicals under LFP conditions, a mixed-order kinetic model that incorporates both second-order and pseudo-first-order kinetics was applied to fit the obtained kinetic profile of the α-aminoalkyl radical **R1**. For the time evolution of the forming alkyl radical, a first-order ascending and mixed-order descending kinetic model were employed to fit the entire kinetic curve. As shown in Figure 2C, the apparent first-order rates (k_{obs}) for the decay of the aminoalkyl radical and the rise of the alkyl radical (7.2×10^4 s^{-1} and 6.6×10^4 s^{-1}, respectively) exhibit good consistency. This serves as a solid basis for quantitative kinetic study on the XAT reactivities of the α-aminoalkyl radicals.

Remarkably, the obtained k_{obs} of approximately 7×10^4 s^{-1} in the presence of 10 mM of alkyl iodide **2** revealed a k_{XAT} between **R1** and **2** of 7×10^6 M^{-1}s^{-1} at maximum, deviating significantly from the anticipated k_{XAT} value at a level of 10^8 M^{-1}s^{-1}.[15] To further quantify the second-order rate constant for the XAT process, we needed to make direct comparisons between the reported k_{XAT} of **R1** and the ones measured by EPR.

Determination of XAT Rate Constants by EPR. A series of kinetic measurements were conducted using U-PSD TREPR, which involved four different α-aminoalkyl radicals: **R1**, **R3**, **R4**, and **R5** (Figure 3). Among them, the second-order rate constants of two individual XAT reactions (**R1** + **3** and **R5** + **3**) have been previously measured using TA spectroscopy.

Gratifyingly, in all cases studied, the α-aminoalkyl radicals exhibited well-resolved transient EPR spectra, which allowed for accurate kinetic measurement by following their characteristic peaks. The transient EPR spectra of **R1** (Figure 3A) and **R4** (Figure 3C) showed a clear E/A polarized pattern resulting from F-pair polarization, aligning with their short lifespans. On the contrary, the spectra of **R3** (Figure 3B) and **R5** (Figure 3D) reassembled thermal equilibrium spin states with

https://doi.org/10.1021/jacs.4c09792
J. Am. Chem. Soc. 2024, 146, 25860−25869

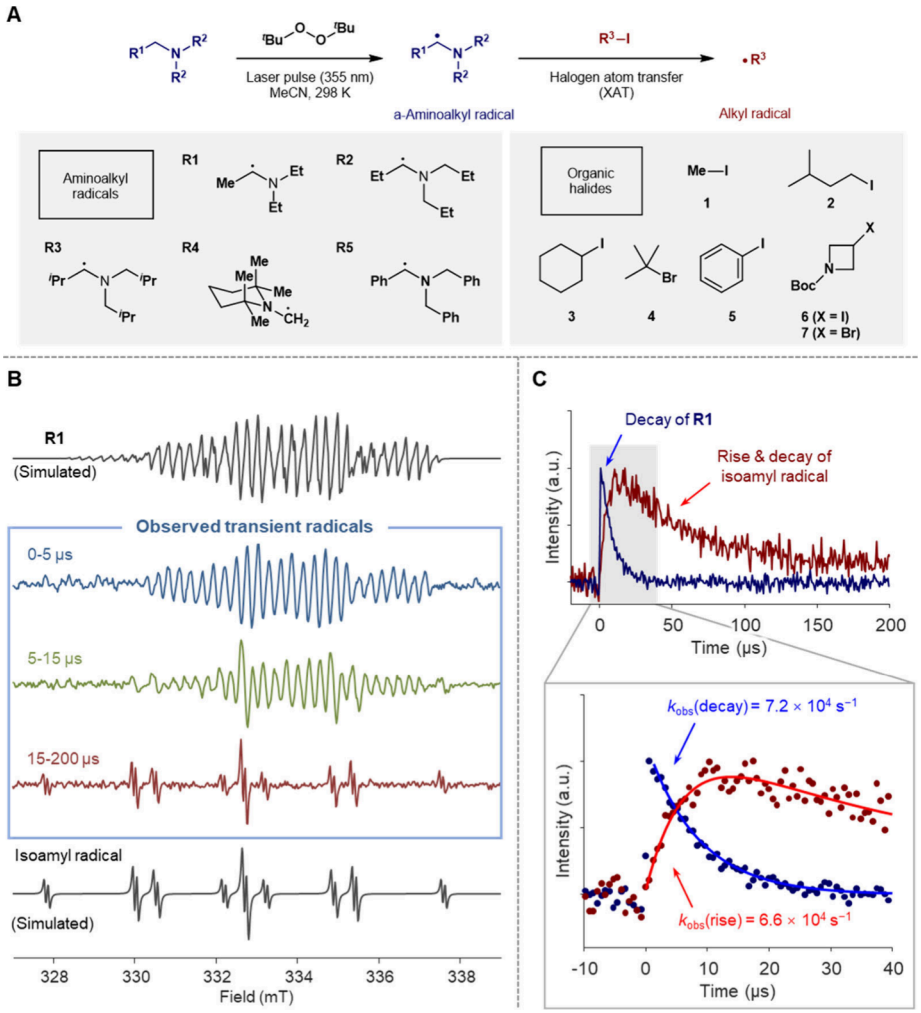

Figure 2. Direct observation of the XAT process of α-aminoalkyl radicals by U-PSD TREPR. (**A**) The model XAT system studied in this work. (**B**) Representative TREPR spectra (X-band, 9.33 GHz) of the XAT process of **R1** with **2**. From top to bottom: simulated spectrum of **R1** (black); acquired spectra with different delays (blue, green, and red); simulated spectrum of isoamyl radical (black). (**C**) The kinetic profiles of the XAT process of **R1** with **2** (10 mM) in MeCN. The expanded subfigure shows the nonlinear fitting of the kinetic traces.

neglectable F-pair polarization, which was consistent with their prolonged lifespans owing to steric hindrance and conjugate stabilization, respectively.

By increasing the concentrations of organic halides, obvious changes in the decay rates of **R1**, **R3**, and **R4** were observed. This revealed substantial quenching of the aminoalkyl radical by organic iodides, and the pseudo first-order rate constants (k_{obs}) were obtained by nonlinear fitting of the kinetic traces using a mixed-order kinetic model incorporating both second-order and pseudo-first-order descending. The second-order XAT rate constants (k_{XAT}) were determined by the linear regression of the obtained k_{obs} and the concentrations of organic halides. Following this procedure, we obtained the k_{XAT} between **R1** and **3** (4.2 × 10^6 M^{-1}s^{-1}, Figure 3A), **R3** and **5** (1.5 × 10^4 M^{-1}s^{-1}, Figure 3B), and **R4** and **1** (7.6 × 10^4 M^{-1}s^{-1}, Figure 3C). However, rather unexpectedly, **R5** derived from tribenzylamine exhibits negligible XAT reactivity with alkyl iodide **3** (k_{XAT} < 10^2 M^{-1}s^{-1}, Figure 3D), and the decay kinetics of **R5** were found to be predominantly second-order in the presence of **3** with various concentrations.

It is clear that the k_{XAT} measured by EPR is inconsistent with the reported ones. For the reaction between **R1** and **3**, the k_{XAT} determined in this work (4.2 × 10^6 M^{-1}s^{-1}) was 2 orders of magnitude smaller than the reported value (3.6 × 10^8 M^{-1}s^{-1}). For the reaction between **R5** and **3**, our results indicated a lack of reactivity (k_{XAT} < 10^2 M^{-1}s^{-1}), while the previous work suggested a reasonable reactivity (k_{XAT} = 1.2 × 10^4 M^{-1}s^{-1}).[15] This contradiction implies that the XAT reactivity profile of α-aminoalkyl radicals deserves a more careful reinvestigation.

2. Cross-Validation Studies Using TA Spectroscopy. The notable discrepancy in the measured XAT rate constants for **R1** and **R5** between our study and previous reports necessitated an investigation into the underlying reasons. To address this, we performed cross-validation by reproducing the TA measurements to determine the XAT rate constants of **R1** and **R5** following the established procedures (Figure 4). In these experiments, **R1** and **R5** were generated in situ by the laser flash photolysis (LFP) of di-*tert*-butyl peroxide (DTBP) in the presence of the corresponding amine. The progress of the XAT reactions was monitored using transient absorption (TA) spectroscopy.

*XAT Rate Constant between **R1** and **3**.* In previous studies, the reaction kinetics of the α-aminoalkyl radical **R1** with alkyl iodide **3** were investigated using a probe protocol employing methyl viologen (MV^{2+}) as the probe (Figure 4A).[15,25] The second-order rate constant of the XAT process can be

https://doi.org/10.1021/jacs.4c09792
J. Am. Chem. Soc. 2024, 146, 25860−25869

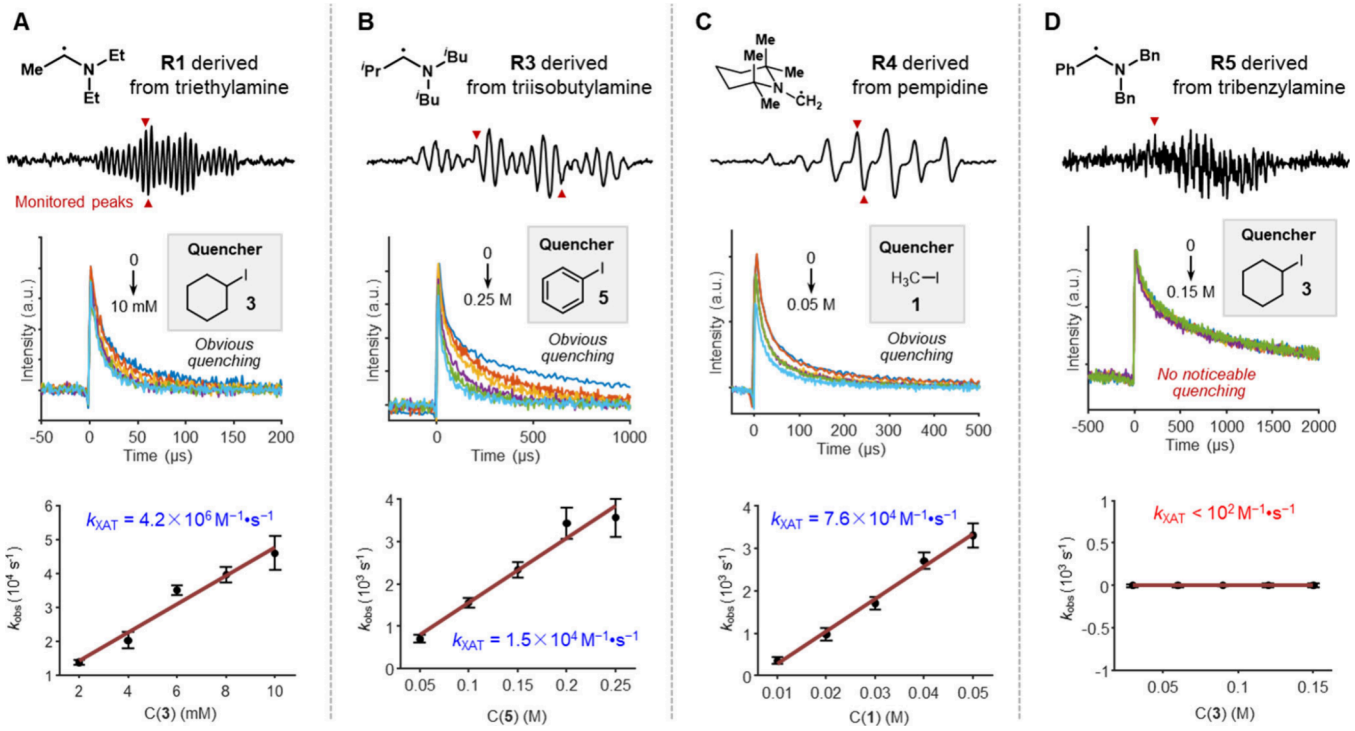

Figure 3. Determination of the XAT rate constants of some α-aminoalkyl radicals by U-PSD TREPR. (**A**) Quenching of **R1** by **3**. (**B**) Quenching of **R3** by **5**. (**C**) Quenching of **R4** by **1**. (**D**) Quenching of **R5** by **3**.

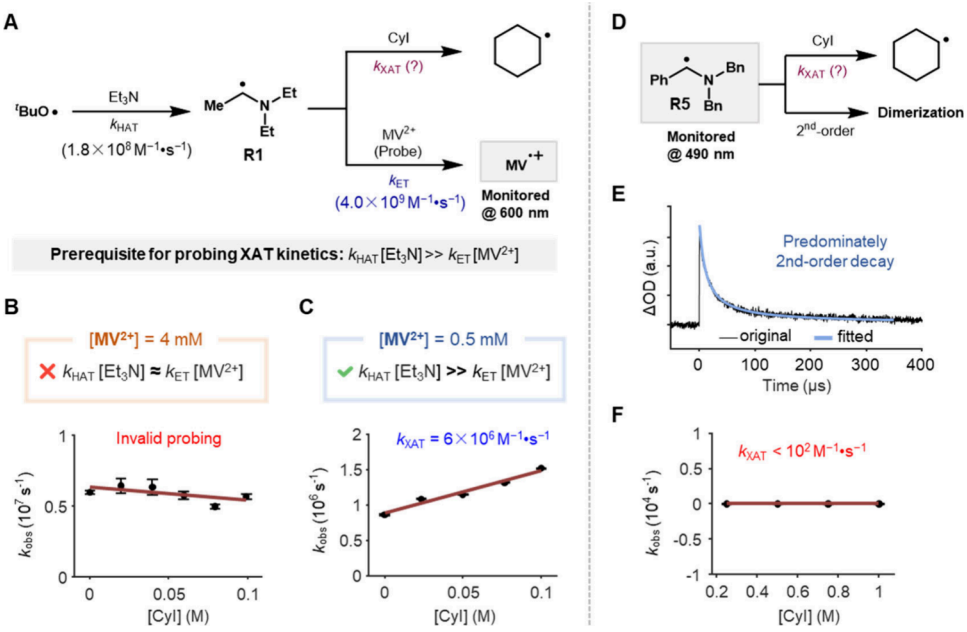

Figure 4. TA spectroscopic measurements. (**A**) Prerequisite for probing the kinetics of **R1** with MV^{2+}. (**B**) Ineffective probing with reported concentrations of MV^{2+}. (**C**) A k_{XAT} of 6×10^6 $M^{-1}s^{-1}$ was measured with a lower concentration of MV^{2+}. (**D**) Direct observation of **R5** with TA. (**E**) Typical kinetic curve of **R5**. (**F**) Negligible quenching of **R5** by **3**.

determined by correlating the build-up kinetics of $MV^{\bullet+}$ with the concentrations of the added **3**. Using this method, Leonori and co-workers obtained a k_{XAT} of 3.6×10^8 $M^{-1}s^{-1}$ with [**3**] ranging from 0 to 10 mM.

When attempting to reproduce this measurement, we realized that certain prerequisite must be met to obtain a reliable second-order rate constant for the XAT process applying this probe method. Specifically, the formation of the aminoalkyl radical must proceed more rapidly compared to the subsequent single electron transfer (SET) between **R1** and MV^{2+} (Figure 4A, and see SI for detailed discussions). Therefore, we first determined the rate constant for the SET step by TA spectroscopy, and the result indicated a diffusion-controlled SET step ($k_{ET} = 4.0 \times 10^9$ $M^{-1}s^{-1}$, see section 6 in the Supporting Information). As the HAT rate constant for the reaction between ^{t}BuO• and Et_3N has been reported to be 1.8×10^8 $M^{-1}s^{-1}$,[26] to meet the kinetic requirement for valid probing of the kinetics of **R1**, [MV^{2+}] must be at least 2 orders

https://doi.org/10.1021/jacs.4c09792
J. Am. Chem. Soc. 2024, 146, 25860−25869

A

k_{XAT} ($M^{-1}•s^{-1}$)	R1	R2	R3	R4	R5	$Et_3Si•$	$^nBu_3Sn•$
1	4.0×10^6	4.8×10^6	4.8×10^5	7.0×10^4	$<10^2$	8×10^9	4×10^9
2	6.5×10^6	7.4×10^6	6.4×10^5	2.3×10^5	$<10^2$	—	—
3	4.2×10^6	4.4×10^6	—	1.2×10^5	$<10^2$	—	—
4	3.0×10^4	2.6×10^4	7.4×10^3	8.7×10^2	—	5×10^8	1×10^8
5	—	—	1.5×10^4	9.7×10^3	$<10^2$	—	—
6	7.8×10^7	—	—	9.6×10^6	$<10^2$	—	—
	Determined in this work					Reported	

B

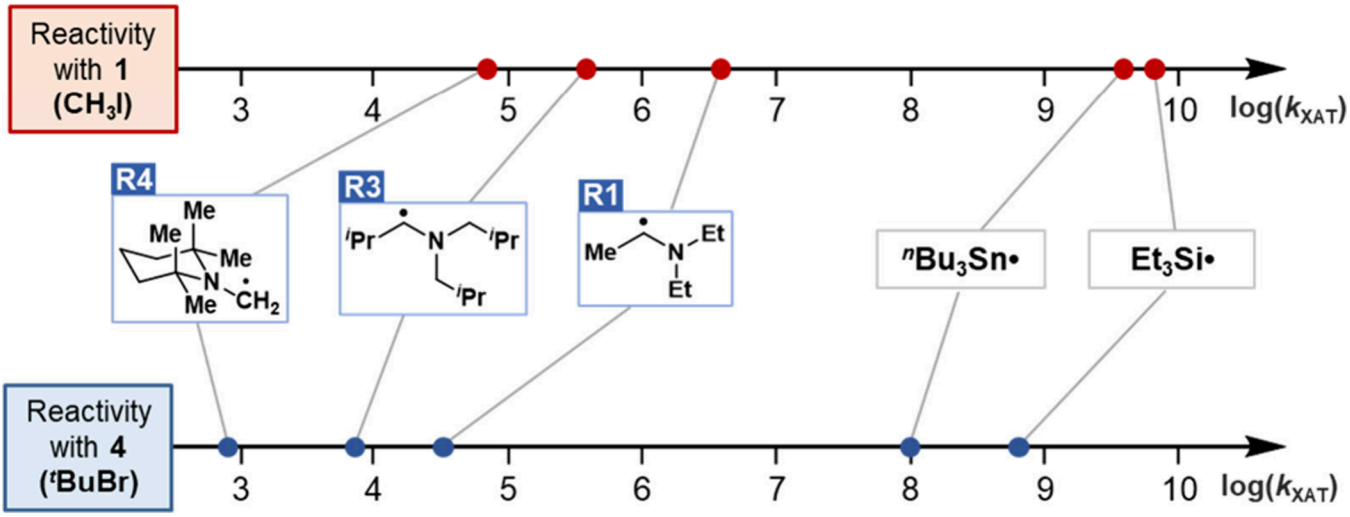

Figure 5. XAT reactivity of α-aminoalkyl radicals. (**A**) Rate constants for the XAT reactions between various α-aminoalkyl radicals and organic halides. (**B**) XAT reactivity scale based on the kinetic data with halides **1** (red dots) and **4** (blue dots).

of magnitude lower than [Et_3N]. However, the test conditions reported by Leonori and co-workers ([Et_3N] = 100 mM and [MV^{2+}] = 4 mM) failed to satisfy this prerequisite. In this case, the acquired kinetic profiles of $MV^{•+}$ could not reflect the actual kinetics of the XAT step. This was verified by repeating the measurement with [MV^{2+}] = 4 mM, in which the dependence of k_{obs} on [**3**] was not observed within a large concentration range (0−100 mM) and only fluctuations due to experimental errors were observed (Figure 4B).

On the contrary, when [MV^{2+}] was decreased to 0.5 mM, a good linear correlation between k_{obs} and [**3**] was observed, and the k_{XAT} was determined to be 6×10^6 $M^{-1}s^{-1}$, which is in excellent agreement with the k_{XAT} measured by EPR (Figure 4C).

*XAT Rate Constant between **R5** and **3**.* To further validate the reported k_{XAT} of **R5**, the reported TA measurements were reproduced (Figure 4D). By directly monitoring the decay of **R5** at 490 nm, we observed predominantly second-order decay kinetics with omittable first-order contribution, even in the presence of a high concentration of **3** (Figure 4E). This aligned well with our TREPR results, and challenged the data processing procedure used in Leonori's work to simply fit the decay kinetics to a monoexponential model with an offset.[15]

To extract a possible value of k_{XAT}, we applied mixed-order kinetic model consisting of both second-order and pseudo-first-order kinetics. However, the obtained pseudo-first-order component was negligible, and thus the k_{XAT} was determined to be $< 10^2$ $M^{-1}s^{-1}$ (Figure 4F). This result challenges the reported value of 1.2×10^4 $M^{-1}s^{-1}$, but is in excellent agreement with our EPR result.

https://doi.org/10.1021/jacs.4c09792
J. Am. Chem. Soc. 2024, 146, 25860−25869

The cross-validation experiment further confirms the authenticity of the results obtained using the U-PSD TREPR method and disproves the kinetic data for aminoalkyl radicals from the previous study. Therefore, it would be valuable to establish a more accurate and extensive XAT reactivity scale using the TREPR method.

3. The XAT Reactivity Profile of α-Aminoalkyl Radicals Determined by U-PSD TREPR. Using the U-PSD TREPR technique, a compelling XAT reactivity profile that encompasses a broader scope of α-aminoalkyl radicals **R1**−**R5** and organic halides **1**−**6** was obtained (Figure 5A). The determined k_{XAT} showed that the α-aminoalkyl radicals are significantly less reactive than silicon[27−29] and tin[30] radicals.

Effect of Organic Halide Structure. The primary alkyl iodide is typically more reactive than iodomethane (e.g., k_{XAT} = 2.3×10^5 $M^{-1}s^{-1}$ versus 7.0×10^4 $M^{-1}s^{-1}$ for **R4** with **2** and **1**, respectively). Cyclohexyl iodide exhibits similar reactivity to primary alkyl iodide in XAT reactions with various α-aminoalkyl radicals. In addition, another secondary alkyl halide, 2-iodopropane, shows a k_{XAT} of 1.9×10^7 $M^{-1}s^{-1}$ with **R1**, about 5 times more reactive than **3**, probably owing to the better stabilization of the XAT transition state (TS) due to enhanced β-C-H hyperconjugation without conformational constraints. Iodobenzene is remarkably less reactive than alkyl iodides (k_{XAT} = 1.5×10^4 $M^{-1}s^{-1}$ versus 4.8×10^5 $M^{-1}s^{-1}$ for **R3** with **5** and **1**, respectively), which is in agreement with the reactivity trends observed in classical XAT reactions.[28]

Notably, when using alkyl iodide **6**, which has an electron-deficient and strained alkyl group, a substantial increase in XAT reactivity was observed. We reasoned that, the electron-deficient nature of the amide group enhances the radical stability of the product radical through a "W" type interaction[31] evidenced by the corresponding HFSs of the nitrogen atom (a_N = 0.12 mT, see SI for details, Figure S10), thereby boosting the driving force of the XAT process. Additionally, the electron-withdrawing property aligns with the polar effect, further reducing the energy barrier. This could elucidate why this specific alkyl halide is widely utilized as a favored substrate in synthetic studies.[21−23]

Effect of α-Aminoalkyl Radical Structure. It was found that, **R1** and **R2** exhibit comparable reactivities due to similarity in structures and steric hindrance. For comparison, Me_2NCH_2• derived from Me_3N exhibited a k_{XAT} of 4.7×10^6 $M^{-1}s^{-1}$, comparable with **R1** and **R2**. This indicated that the structure of normal alkyl substituent in α-aminoalkyl radicals exerts a minor influence on the XAT reactivity. The more sterically congested radicals, **R3** and **R4**, exhibit reactivities that are generally 1−2 orders of magnitude lower toward the same alkyl halide.

The tribenzylamine-derived **R5** shows no XAT reactivity with all organic halides tested within the detection limits of the U-PSD TREPR method (k_{XAT} < 10^2 $M^{-1}s^{-1}$), even with the most reactive alkyl iodide **6**. This indicated that, the previously reported k_{XAT} values of 10^3 to 10^4 $M^{-1}s^{-1}$ for the reactions of **R5** with halides **3** and **5**[15] need to be corrected. Notably, the determined k_{XAT} of < 10^2 $M^{-1}s^{-1}$ is in agreement with the reported DFT computational results that the XAT reaction of **R5** with **3** showed an activation Gibbs free energy of over 20 kcal/mol.[32]

Another factor worthy of note is the lifespan of the α-aminoalkyl radicals. **R3** and **R5** exhibit longer lifespans (remain detectable even after 1 ms) compared with other α-aminoalkyl radicals studied (diminished within hundreds of μs), owing to steric hindrance and conjugate stabilization, respectively. Considering that **R3** exhibits only slightly lower reactivity compared to **R1** and **R2**, while **R5** displays significantly lower reactivity, the longer-lived yet still reactive **R3** may have a higher potential for synthetic applications in XAT reactions.

The XAT Reactivity Scale. These extensive kinetic data allowed us to conduct a fair comparison of the XAT reactivity of α-aminoalkyl radicals with that of traditional tin and silicon radicals (Figure 5B). Methyl iodide (**1**) and *tert*-butyl bromide (**4**) were selected as standard compounds, as they can roughly represent the upper and lower limits of alkyl halide XAT reactivity, respectively, and their k_{XAT} values with Et_3Si• and nBu_3Sn• have been previously documented.[27−30] With both alkyl halides, α-aminoalkyl radicals were found to be 10^3 to 10^5 times less reactive than the tributyltin radical. Based on these data, a trend of the XAT reactivity could be described as Et_3Si• > nBu_3Sn• ≫ **R1** ≈ **R2** ≈ Me_2NCH_2• > **R3** > **R4** ≫ **R5**.

Correlation of the XAT Reactivity Scale to the Reaction Outcomes. The established XAT reactivity scale could be confirmed by synthetic reaction outcomes. The dehalogenation reaction of an alkyl iodide in the presence of an amine, $K_2S_2O_8$, and a thiol under thermal conditions was performed following Leonori's procedure (Figure 6).[15] In this reaction system, the

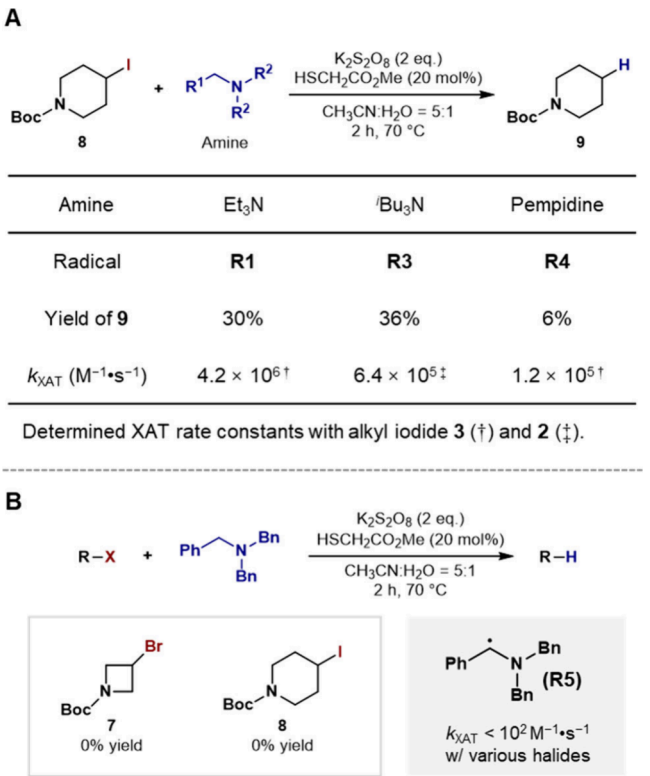

Figure 6. Validation of the XAT reactivity by synthetic experiments. (**A**) XAT reactions of α-aminoalkyl radicals generated by thermal oxidation of various amines. (**B**) XAT reactions of α-aminoalkyl radicals generated by thermal oxidation of tribenzylamine.

α-aminoalkyl radical intermediate is generated through single electron oxidation/deprotonation, maintaining an overall oxidative environment that excludes the SET reduction of the alkyl iodide. Therefore, the formation of the dehalogenation product from alkyl iodide serves as a perfect indicator for the XAT reactivity of the corresponding α-aminoalkyl radical.

https://doi.org/10.1021/jacs.4c09792
J. Am. Chem. Soc. 2024, 146, 25860−25869

Our results showed that triethylamine, triisobutylamine, and pempidine, corresponding to radicals **R1**, **R3**, and **R4**, produced detectable yields of dehalogenation product **9** from iodide **8** (Figure 6A), correlating well with their k_{XAT} of > 10^5 $M^{-1}s^{-1}$. On the contrary, tribenzylamine, the precursor of radical **R5**, showed no reactivity toward either activated bromide **7** or iodide **8** (Figure 6B), which is not unexpected considering its k_{XAT} of < 10^2 $M^{-1}s^{-1}$. The correlation between the chemical yields and the established reactivity scale indicates that the established XAT reactivity scale is reliable.

This finding also highlights the need for a reevaluation of mechanistic interpretations regarding the XAT activity of α-aminoalkyl radicals. Previous experimental studies have demonstrated the transformation of alkyl bromides to the corresponding radicals in a photoredox system involving tribenzylamine and 4CzIPN. However, the reaction between **R5** and **7** showed a neglectable reactivity with k_{XAT} of < 10^2 $M^{-1}s^{-1}$ (Table S35), and under thermochemical conditions, dehalogenation of **7** did not occur with **R5** (Figure 6B), suggesting a potentially different mechanism other than XAT for alkyl halide activation under photoredox conditions. Recently, there have been extensive discussions on the noninnocent role of the photocatalyst 4CzIPN in dehalogenation reactions, indicating that the 4CzIPN radical anion can reduce organic halides under visible light irradiation.[33] Therefore, in the seminal photoredox system with both tribenzylamine and 4CzIPN, it is possible that tribenzylamine functions as a sacrificial electron donor, or that other active species were generated upon the decomposition of tribenzylamine under these conditions.

4. Mechanistic Analysis of the XAT Process. In the previous report, the kinetic polar effect was employed to explain the exceptionally high XAT reactivity of the α-aminoalkyl radical comparable to classical tin radicals. However, our established XAT reactivity scale clearly demonstrates that α-aminoalkyl radicals exhibit substantially lower reactivity than the classical tin and silicon radicals, contradicting the initial expectations. Therefore, a detailed analysis of the XAT reaction mechanism of α-aminoalkyl radicals is necessary. This will help elucidate the revised reactivity trends and provide a comprehensive assessment of the polar effect induced by the amino group.

Solvent Effect. To assess the polarity of the XAT TS, we investigated the solvent effect of the XAT reaction between **R1** and **3**. The XAT rate constants were measured in an array of solvents with different polarities, including ethyl acetate, acetone, and acetonitrile−water mixtures (Figure 7A). The Dimroth−Reichardt parameter ($E_T(30)$)[34] was used as a measure of solvent polarity, and a plot of k_{XAT} versus $E_T(30)$ was used to analyze the solvent effect on the XAT process (Figure 7B). Unexpectedly, it was observed that solvent polarity had only a marginal influence on the XAT process, and a slight negative correlation between k_{XAT} and solvent polarity was observed. It indicated that the XAT TS does not get more stabilized in a more polar reaction medium, corresponding to a minimal extent of charge separation in the TS. We postulate that the ionization step leading to the iminium structure either does not contribute to the critical XAT TS or occurs at a late stage, resulting in minimal influence on the overall activation energy barrier.

This is in stark contrast to the significantly greater promotional effect of solvent polarity on conventional polar C-X bond cleavage reactions,[35] as well as in the XAT reactions

A

Solvent	$E_T(30)$ (kcal/mol)	k_{XAT} ($M^{-1}•s^{-1}$)
EtOAc	38.1	5.2 × 10^6
Acetone	42.1	2.9 × 10^6
MeCN	45.6	4.2 × 10^6
MeCN + 5% H_2O	51.8	3.6 × 10^6
MeCN + 10% H_2O	53.4	3.3 × 10^6
MeCN + 15% H_2O	53.9	3.1 × 10^6

B

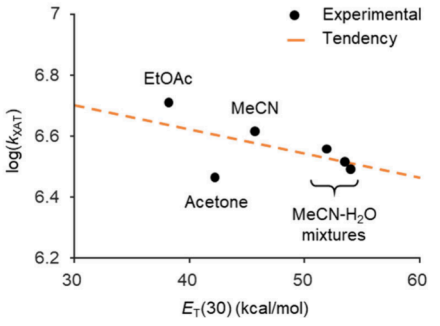

Figure 7. Solvent effect of the XAT reaction. (**A**) Measuring the k_{XAT} between **R1** and **3** in various solvents. (**B**) Correlation between the measured k_{XAT} and $E_T(30)$ of the solvents.

between α-aminoalkyl radicals and highly electron-deficient polyhalomethanes, where dissociative electron transfer was believed to occur.[13] Therefore, we suggest describing the XAT process between α-aminoalkyl radicals and normal organic halides as an atom transfer-like reaction that does not involve a highly polarized dissociative TS.

Valence Bond State Correlation Diagram (VBSCD) Analysis. We then compared the XAT reactivities of α-aminoalkyl radicals and normal alkyl radicals to understand the effect of the amino group on the XAT process (Figure 8). To make a fair comparison, we used the XAT rate constants of a primary alkyl radical ($^nC_{11}H_{23}•$) and an α-aminoalkyl radical derived from Me_3N ($Me_2NCH_2•$) measured by U-PSD TREPR employing the same alkyl iodide **3**. The XAT reactivity of the primary alkyl radical was found to be in good agreement with previously reported values,[16] with a k_{XAT} of 1.4 × 10^5 $M^{-1}s^{-1}$. For the α-aminoalkyl radical derived from trimethylamine, a k_{XAT} of 4.7 × 10^6 $M^{-1}s^{-1}$ was obtained. It is evidenced that the α-aminoalkyl radical indeed exhibits greater XAT reactivity than the primary alkyl radical, albeit with a marginal increase that is significantly less pronounced than anticipated.

The VBSCD approach was utilized to rationalize the reactivity difference between the two XAT reactions. The state correlation diagrams[36] are depicted in Figure 8. The interplay of the primary Heitler-London (HL) structures and the primary ionic structures shows the origin of the barrier of the XAT process. Specifically, the energy profile along the HL states illustrates the variations in radical stabilization energy (RSE) between the reactant radical and the product radical, whereas the energy profile of the ionic states indicates the contribution of polar effects.

https://doi.org/10.1021/jacs.4c09792
J. Am. Chem. Soc. 2024, 146, 25860−25869

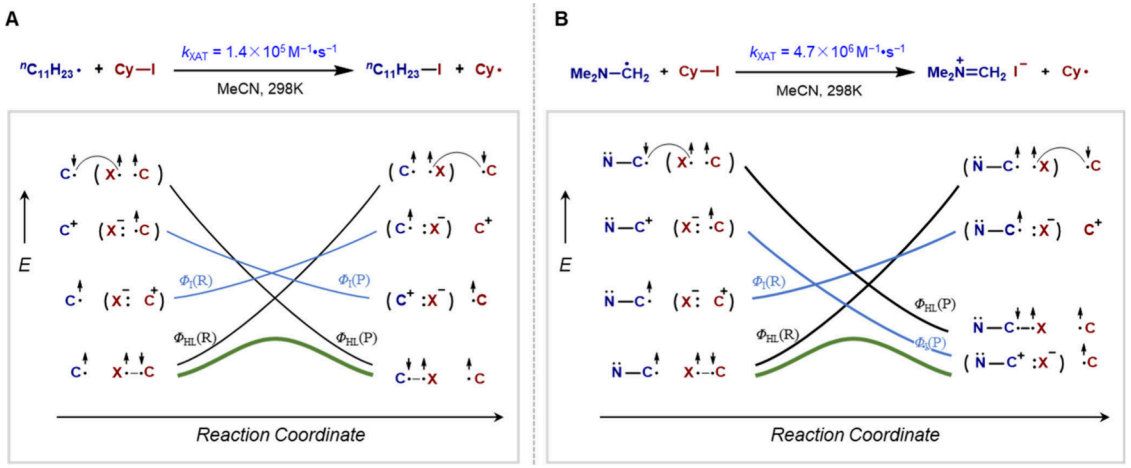

Figure 8. VBSCD analysis on the XAT reactions involving an α-aminoalkyl radical and a conventional alkyl radical. (**A**) The XAT reaction between $^{n}C_{11}H_{23}\bullet$ and **3**. (**B**) The XAT reaction between $Me_2NCH_2\bullet$ and **3**.

The XAT between alkyl radical and alkyl iodide can be considered an intrinsic reaction with symmetrical energy profiles for each electronic configurational state, resulting in almost zero enthalpic effect. The contribution of ionic structures of the C−I bond in alkyl iodide is not significant, so the energy levels of the ionic states are well above those of the HL states, making polar effects insignificant in this process (Figure 8A).

However, the XAT reaction between α-aminoalkyl radical and alkyl iodide differs. Beginning with the HL structure of the reactants (labeled as $\Phi_{HL}(R)$), the C−I bond of alkyl iodide breaks along the reaction coordinate, and an unfavorable enthalpic effect arises from the HL structures of products as the radical stabilization energy (RSE) of the initial α-aminoalkyl radical surpasses that of the generated alkyl radical. On the other hand, the nitrogen lone pair contributes to the stabilization of the emerging positive charge on the α-carbon in the ionic structures, leading to a favorable ionic enthalpic contribution. This results in inverted energy levels of the corresponding HL and ionic structures of the product ($\Phi_{HL}(P)$ and $\Phi_I(P)$, respectively). The overall interplay of these two opposing effects results in less stabilization than expected, elucidating the marginal driving force of the XAT process and the minor stabilization effect on the transition state (Figure 8B).

Previous investigations have attributed the postulated exceptionally high XAT reactivity of α-aminoalkyl radicals to polar effects.[15] However, our studies have revealed that α-aminoalkyl radicals derived from common amines exhibit only a modestly higher reactivity compared to primary alkyl radicals, which could be well rationalized by the VBSCD approach. Based on this analysis, it becomes clear why α-aminoalkyl and α-oxyalkyl radicals do not exhibit a significant kinetic advantage over alkyl radicals in XAT reactions, as previously suggested by DFT calculations.[37]

CONCLUSION

In this study, the XAT reaction between α-aminoalkyl radicals and normal alkyl halides has been carefully examined using our developed U-PSD TREPR technique. This radical-specific method allowed us to directly observe the XAT process through EPR spectroscopy and offered an approach to studying both the fine structures and the kinetics of radicals. A series of second-order rate constants for the XAT reactions between α-aminoalkyl radicals and organic halides were determined, some of which were cross-validated using TA spectroscopy.

The key discovery of this study is that the reactivity of these radicals in XAT reactions is significantly lower (by 3−5 orders of magnitude) than that of tin and silicon radicals, and only slightly higher than that of alkyl radicals. Based on the determined rate constants, we propose a general trend for the XAT reactivity as trialkylsilicon radicals > trialkyltin radicals ≫ alkyl substituted α-aminoalkyl radicals > bulky alkyl substituted α-aminoalkyl radicals ≈ primary alkyl radical ≫ α-aminobenzyl radicals. This challenges the previously held belief that α-aminoalkyl radicals exhibit a reactivity profile similar to classical tin radicals. Our findings establish a reliable XAT reactivity profile for α-aminoalkyl radicals, laying the groundwork for the rational design of XAT reactions. Given the increasing prominence of XAT reactions involving α-aminoalkyl radicals in state-of-the-art research, this study timely corrects the reactivity scale of these radicals, which is essential for mechanistic understanding and reaction design.

ASSOCIATED CONTENT

Supporting Information

The Supporting Information is available free of charge at https://pubs.acs.org/doi/10.1021/jacs.4c09792.

Details for experimental procedures, spectra simulation, kinetic fitting, and compound characterization (PDF)

AUTHOR INFORMATION

Corresponding Authors

Lei Jiao − *Center of Basic Molecular Science (CBMS), Department of Chemistry, Tsinghua University, Beijing 100084, China;* orcid.org/0000-0002-8465-1358; Email: leijiao@mail.tsinghua.edu.cn

Xingwei Guo − *Center of Basic Molecular Science (CBMS), Department of Chemistry, Tsinghua University, Beijing 100084, China;* orcid.org/0000-0002-5461-0360; Email: xingwei_guo@mail.tsinghua.edu.cn

Authors

Weiqun Suo − *Center of Basic Molecular Science (CBMS), Department of Chemistry, Tsinghua University, Beijing 100084, China*

Jian-Qing Qi − *Center of Basic Molecular Science (CBMS), Department of Chemistry, Tsinghua University, Beijing 100084, China*; orcid.org/0000-0001-5042-6315

Jing Liu − *Center of Basic Molecular Science (CBMS), Department of Chemistry, Tsinghua University, Beijing 100084, China*

Songtao Sun − *Center of Basic Molecular Science (CBMS), Department of Chemistry, Tsinghua University, Beijing 100084, China*

Complete contact information is available at: https://pubs.acs.org/10.1021/jacs.4c09792

Author Contributions

⊥W.S. and J.-Q.Q. contributed equally.

Notes

The authors declare no competing financial interest.

■ ACKNOWLEDGMENTS

The authors thank Prof. H. Mayr for comments on the manuscript and Prof. M.-T. Zhang for helpful discussions. This work was supported by Tsinghua University Dushi Program.

■ REFERENCES

(1) Chatgilialoglu, C.; Ferreri, C.; Landais, Y.; Timokhin, V. I. Thirty Years of (TMS)3SiH: A Milestone in Radical-Based Synthetic Chemistry. *Chem. Rev.* **2018**, *118* (14), 6516−6572.

(2) Neumann, W. P. Tri-n-Butyltin Hydride as Reagent in Organic Synthesis. *Synthesis* **1987**, *1987* (8), 665−683.

(3) Juliá, F.; Constantin, T.; Leonori, D. Applications of Halogen-Atom Transfer (XAT) for the Generation of Carbon Radicals in Synthetic Photochemistry and Photocatalysis. *Chem. Rev.* **2022**, *122* (2), 2292−2352.

(4) Wu, Z.; Pratt, D. A. Radical Approaches to C−S Bonds. *Nat. Rev. Chem.* **2023**, *7* (8), 573−589.

(5) Sumida, Y.; Ohmiya, H. Direct Excitation Strategy for Radical Generation in Organic Synthesis. *Chem. Soc. Rev.* **2021**, *50* (11), 6320−6332.

(6) Prier, C. K.; Rankic, D. A.; MacMillan, D. W. C. Visible Light Photoredox Catalysis with Transition Metal Complexes: Applications in Organic Synthesis. *Chem. Rev.* **2013**, *113* (7), 5322−5363.

(7) Bell, J. D.; Murphy, J. A. Recent Advances in Visible Light-Activated Radical Coupling Reactions Triggered by (i) Ruthenium, (Ii) Iridium and (Iii) Organic Photoredox Agents. *Chem. Soc. Rev.* **2021**, *50* (17), 9540−9685.

(8) Pitre, S. P.; Overman, L. E. Strategic Use of Visible-Light Photoredox Catalysis in Natural Product Synthesis. *Chem. Rev.* **2022**, *122* (2), 1717−1751.

(9) Le, C.; Chen, T. Q.; Liang, T.; Zhang, P.; MacMillan, D. W. C. A Radical Approach to the Copper Oxidative Addition Problem: Trifluoromethylation of Bromoarenes. *Science* **2018**, *360* (6392), 1010−1014.

(10) Chan, A. Y.; Perry, I. B.; Bissonnette, N. B.; Buksh, B. F.; Edwards, G. A.; Frye, L. I.; Garry, O. L.; Lavagnino, M. N.; Li, B. X.; Liang, Y.; Mao, E.; Millet, A.; Oakley, J. V.; Reed, N. L.; Sakai, H. A.; Seath, C. P.; MacMillan, D. W. C. Metallaphotoredox: The Merger of Photoredox and Transition Metal Catalysis. *Chem. Rev.* **2022**, *122* (2), 1485−1542.

(11) Lalevée, J.; Graff, B.; Allonas, X.; Fouassier, J. P. Aminoalkyl Radicals: Direct Observation and Reactivity toward Oxygen, 2,2,6,6-Tetramethylpiperidine-N-Oxyl, and Methyl Acrylate. *J. Phys. Chem. A* **2007**, *111* (30), 6991−6998.

(12) Lalevée, J.; Allonas, X.; Fouassier, J. P. Halogen Abstraction Reaction between Aminoalkyl Radicals and Alkyl Halides: Unusual High Rate Constants. *Chem. Phys. Lett.* **2008**, *454* (4), 415−418.

(13) Lalevée, J.; Fouassier, J. P.; Blanchard, N.; Ingold, K. U. Reaction between Aminoalkyl Radicals and Akyl Halides: Dehalogenation by Electron Transfer? *Chem. Phys. Lett.* **2011**, *511* (1), 156−158.

(14) Neff, R. K.; Su, Y.-L.; Liu, S.; Rosado, M.; Zhang, X.; Doyle, M. P. Generation of Halomethyl Radicals by Halogen Atom Abstraction and Their Addition Reactions with Alkenes. *J. Am. Chem. Soc.* **2019**, *141* (42), 16643−16650.

(15) Constantin, T.; Zanini, M.; Regni, A.; Sheikh, N. S.; Juliá, F.; Leonori, D. Aminoalkyl Radicals as Halogen-Atom Transfer Agents for Activation of Alkyl and Aryl Halides. *Science* **2020**, *367* (6481), 1021−1026.

(16) Newcomb, M.; Sanchez, R. M.; Kaplan, J. Fast Halogen Abstractions from Alkyl Halides by Alkyl Radicals. Quantitation of the Processes Occurring in and a Caveat for Studies Employing Alkyl Halide Mechanistic Probes. *J. Am. Chem. Soc.* **1987**, *109* (4), 1195−1199.

(17) Coote, M. L.; Lin, C. Y.; Zipse, H. The Stability of Carbon-Centered Radicals. In *Carbon-Centered Free Radicals and Radical Cations*; John Wiley & Sons, Ltd, 2009; pp 83−104.

(18) Pasto, D. J. Radical Stabilization Energies of Disubstituted Methyl Radicals. A Detailed Theoretical Analysis of the Captodative Effect. *J. Am. Chem. Soc.* **1988**, *110* (24), 8164−8175.

(19) Zhang, S.; Zhou, S.; Qi, J.; Jiao, L.; Guo, X. Time-Resolved Electron Paramagnetic Resonance Spectrometer Based on Ultrawide Single-Sideband Phase-Sensitive Detection. *Rev. Sci. Instrum.* **2023**, *94* (8), No. 084101.

(20) Qi, J.-Q.; Suo, W.; Liu, J.; Sun, S.; Jiao, L.; Guo, X. Direct Observation of All Open-Shell Intermediates in a Photocatalytic Cycle. *J. Am. Chem. Soc.* **2024**, *146* (11), 7140−7145.

(21) Caiger, L.; Sinton, C.; Constantin, T.; Douglas, J. J.; Sheikh, N. S.; Julia, F.; Leonori, D. Radical Hydroxymethylation of Alkyl Iodides Using Formaldehyde as a C1 Synthon. *Chem. Sci.* **2021**, *12* (31), 10448−10454.

(22) Zhang, Z.; Górski, B.; Leonori, D. Merging Halogen-Atom Transfer (XAT) and Copper Catalysis for the Modular Suzuki−Miyaura-Type Cross-Coupling of Alkyl Iodides and Organoborons. *J. Am. Chem. Soc.* **2022**, *144* (4), 1986−1992.

(23) Sun, X.; Zheng, K. Electrochemical Halogen-Atom Transfer Alkylation via α-Aminoalkyl Radical Activation of Alkyl Iodides. *Nat. Commun.* **2023**, *14* (1), 6825.

(24) Wood, D. E.; Lloyd, R. V. EPR of Free Radicals in an Adamantane Matrix. I. Aliphatic Aminoalkyl Radicals. *J. Chem. Phys.* **2003**, *53* (10), 3932−3942.

(25) McTiernan, C. D.; Pitre, S. P.; Scaiano, J. C. Photocatalytic Dehalogenation of Vicinal Dibromo Compounds Utilizing Sexithiophene and Visible-Light Irradiation. *ACS Catal.* **2014**, *4* (11), 4034−4039.

(26) Griller, D.; Howard, J. A.; Marriott, P. R.; Scaiano, J. C. Absolute Rate Constants for the Reactions of Tert-Butoxyl, Tert-Butylperoxyl, and Benzophenone Triplet with Amines: The Importance of a Stereoelectronic Effect. *J. Am. Chem. Soc.* **1981**, *103* (3), 619−623.

(27) Chatgilialoglu, C.; Ingold, K. U.; Scaiano, J. C.; Woynar, H. Absolute Rate Constants for Some Reactions Involving Triethylsilyl Radicals in Solution. *J. Am. Chem. Soc.* **1981**, *103* (11), 3231−3232.

(28) Chatgilialoglu, C.; Ingold, K. U.; Scaiano, J. C. Absolute Rate Constants for the Reaction of Triethylsilyl Radicals with Organic Halides. *J. Am. Chem. Soc.* **1982**, *104* (19), 5123−5127.

(29) Chatgilialoglu, C.; Griller, D.; Lesage, M. Rate Constants for the Reactions of Tris(Trimethylsilyl)Silyl Radicals with Organic Halides. *J. Org. Chem.* **1989**, *54* (10), 2492−2494.

(30) Carlsson, D. J.; Ingold, K. U. Kinetics and Rate Constants for the Reduction of Alkyl Halides by Organotin Hydrides. *J. Am. Chem. Soc.* **1968**, *90* (25), 7047−7055.

(31) Gerson, F.; Huber, W. Organic Radicals Centered on One, Two, or Three Atoms. In *Electron Spin Resonance Spectroscopy of Organic Radicals*; John Wiley & Sons, 2003; pp 177−180.
(32) Sanosa, N.; Peñín, B.; Sampedro, D.; Funes-Ardoiz, I. On the Mechanism of Halogen Atom Transfer from C−X Bonds to α-Aminoalkyl Radicals: A Computational Study. *Eur. J. Org. Chem.* **2022**, *2022* (34), No. e202200420.
(33) Chmiel, A. F.; Williams, O. P.; Chernowsky, C. P.; Yeung, C. S.; Wickens, Z. K. Non-Innocent Radical Ion Intermediates in Photoredox Catalysis: Parallel Reduction Modes Enable Coupling of Diverse Aryl Chlorides. *J. Am. Chem. Soc.* **2021**, *143* (29), 10882−10889.
(34) Skwierczynski, R.; Connors, K. Solvent Effects on Chemical Processes. Part 7. Quantitative Description of the Composition Dependence of the Solvent Polarity Measure E T (30) in Binary Aqueous−Organic Solvent Mixtures. *Journal of the Chemical Society, Perkin Transactions 2* **1994**, *0* (3), 467−472.
(35) Wells, P. R. Linear Free Energy Relationships. *Chem. Rev.* **1963**, *63* (2), 171−219.
(36) Shaik, S.; Hiberty, P. C. Valence Bond Theory, Its History, Fundamentals, and Applications: A Primer. In *Reviews in Computational Chemistry*; John Wiley & Sons, Ltd, 2004; pp 1−100.
(37) Itsenko, O.; Norberg, D.; Rasmussen, T.; Långström, B.; Chatgilialoglu, C. Radical Carbonylation with [11C]Carbon Monoxide Promoted by Oxygen-Centered Radicals: Experimental and DFT Studies of the Mechanism. *J. Am. Chem. Soc.* **2007**, *129* (29), 9020−9031.

https://doi.org/10.1021/jacs.4c09792
J. Am. Chem. Soc. 2024, 146, 25860−25869